Tracer Diffusion in Colloidal Gels

Sujin Babu, Jean Christophe Gimel,* and Taco Nicolai

Polymères Colloïdes Interfaces, CNRS UMR6120, Université du Maine, F-72085 Le Mans cedex 9, France

Received: August 7, 2007; In Final Form: October 25, 2007

Computer simulations were done of the mean square displacement (MSD) of tracer particles in colloidal gels formed by diffusion or reaction limited aggregation of hard spheres. The diffusion coefficient was found to be determined by the volume fraction accessible to the spherical tracers (ϕ_a) independent of the gel structure or the tracer size. In all cases, critical slowing down was observed at $\phi_a \approx 0.03$ and was characterized by the same scaling laws reported earlier for tracer diffusion in a Lorentz gas. Strong heterogeneity of the MSD was observed at small ϕ_a and was related to the size distribution of pores.

I. Introduction

Irreversible aggregation of colloidal particles such as proteins,[1] clay,[2] or oil droplets[3] in solution often leads to the formation of a percolating structure that can resist stress. Recently, the colloidal gel[4,5] formation has been studied in detail for diffusion limited cluster aggregation of hard spheres using off-lattice computer simulations.[6,7] The gels have locally a self-similar structure characterized by a fractal dimension and are homogeneous beyond a characteristic length scale that decreases with increasing volume fraction of the particles (ϕ).

The transport properties of tracer particles in colloidal gels obviously depend on the volume fraction of the gels that is accessible to the center of mass of the particles (ϕ_a). The accessible volume, or porosity, depends on the size of the tracers; if the tracers are very small compared to the colloids, ϕ_a is close to $1 - \phi$,[8] but it decreases for a given ϕ with increasing size of the tracers. Consequently, the long time diffusion coefficient (D) of the tracers decreases with increasing ϕ or tracer size and goes to zero at a critical value of ϕ_a. When the accessible volume is small, it consists of randomly branched pores that can be of finite size or else percolate through the system.

It has long been known that transport close to the dynamical arrest can be described in terms of diffusion on a percolating network.[9] The geometrical and transport properties of percolation have been investigated extensively on lattices using computer simulations.[10−12] The diffusion coefficient of particles was found to go to zero at the percolation threshold following a power law: $D \propto \epsilon^{\mu}$, where $\epsilon = (\phi_a - \phi_a^c)/\phi_a^c$ is the relative distance of the accessible volume fraction to the threshold value (ϕ_a^c). Close to the threshold, the mean square displacement (MSD) of the tracers becomes subdiffusive, meaning that the MSD has a power law dependence on time: $\langle r^2 \rangle \propto t^k$, with $k < 1$.[9,13]

In standard lattice simulations, the probability to move between neighboring sites of the network is constant. However, in real systems, the pores have a broad continuous range of channel diameters and therefore the local mobility of tracers varies in space. In order to account for this effect, the lattice model was extended to include a power law distribution of probabilities to move between sites.[10] If the exponent of this power law is less than unity, the mobility over large distances is dominated by the lowest probability, which decreases with increasing distance. For this reason, μ and k are reduced to an extent that depends on the exponent. Two different estimates of μ and k were given for the case of randomly distributed overlapping spherical obstacles, that is, obstacles forming a so-called Lorentz gas, leading to slightly different values of μ and k: 2.38 and 0.36[10] or 2.88 and 0.32.[11]

Recently, detailed off-lattice simulations were reported on the tracer diffusion in porous media formed by a Lorentz gas at different densities very close to the percolation threshold.[13] The aim was to verify the adequacy of the extended lattice model for this system. Anomalous diffusion was observed at the threshold, and the exponents μ and k were found to be consistent with the predictions by Machta et al.[11] The critical value of the accessible volume fraction was $\phi_a^c = 0.0298$, close to values found with other simulations[12] and in experiments on real systems.[14]

However, a Lorentz gas of overlapping spherical obstacles is not a realistic model for particle gels. Here, we investigate the transport in particle gels formed by irreversible aggregation of hard spheres using computer simulations. Two limiting cases are gels formed by diffusion limited aggregation (DLCA) in which a rigid bond is formed at each collision and reaction limited aggregation (RLCA) in which the bond formation probability goes to zero. Irreversible aggregation leads to the formation of self-similar aggregates with a fractal dimension of 1.8 for DLCA and 2.1 for RLCA.[15] When the aggregates have grown to the extent that they fill up the space, they connect into a system spanning structure. Such gels can actually be made, and the diffusion of tracer particles in such systems can be determined experimentally using, for example, confocal laser scanning microscopy[16] or pulsed field gradient NMR.[17] In order to investigate the effect of spatial correlation caused by aggregation, we also studied tracer self-diffusion in systems of frozen randomly distributed hard spheres (FHS).

II. Simulation Method

Gels were simulated by irreversible cluster−cluster aggregation starting from a random distribution of hard spheres with unit diameter until all particles were connected; see ref 4 for details. The diffusion of tracers was simulated by small

* To whom correspondence should be addressed. E-mail: Jean-Christophe.Gimel@univ-lemans.fr.

10.1021/jp076342+ CCC: $40.75
Published on Web 01/03/2008

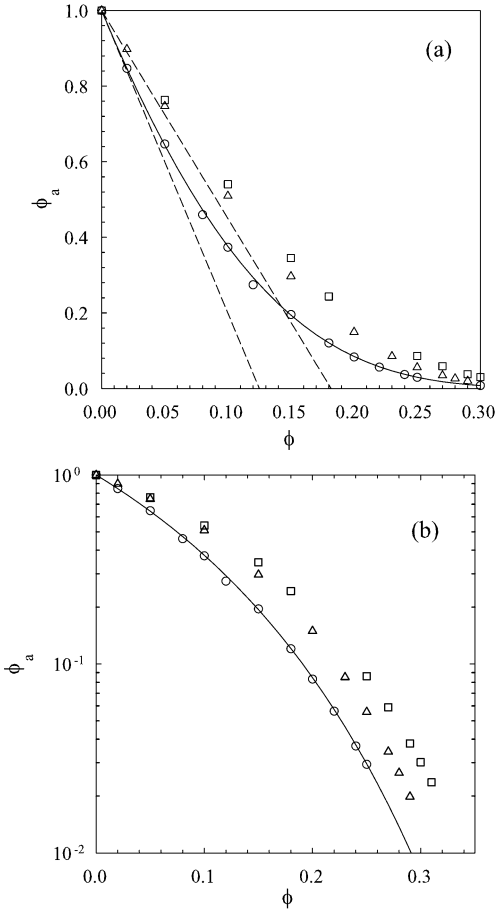

Figure 1. (a) The accessible volume fraction as a function of ϕ for tracer spheres in FHS (circles), DLCA (triangles), and RLCA (squares) gels of spheres with the same diameter as the tracers. The dashed lines represent the limiting low concentration behavior; see text. (b) The same data as part a on a logarithmic scale for ϕ_a. The solid line represents values calculated using the Carnahan−Starling equation, see text.

displacements in a random direction. If the displacement led to overlap, the movement was either refused or truncated at contact. For small MSD, the step size was chosen sufficiently small so that reducing it further had no significant effect on the results. For large MSD, larger step sizes were chosen to speed up the displacement. This did not influence the relative time dependence of the MSD but did result in the wrong absolute values. The correct absolute values were recovered by superposition at smaller MSD with simulations using small step sizes. In a few cases, we used a small step size up to large MSD to verify that this procedure gave the correct results.

The time unit was chosen as the time needed for a tracer to diffuse over its diameter at infinite dilution, which is about 0.4 s for a particle with a diameter of 1 μm in water at room temperature. Simulations were done in a box with length 50 using periodic boundary conditions. We checked for finite size effects by varying the box size, and all results shown here are not influenced by finite size effects. We averaged over several hundred paths of randomly inserted tracers and 10 independent system configurations. ϕ_a was calculated as the probability that a tracer could be randomly inserted without overlap.

III. Results and Discussion

We present first results for the case that the tracer particles have the same diameter as the obstacle particles, after which we discuss the effect of varying the tracer size. In Figure 1, the dependence of ϕ_a is plotted as a function of ϕ for randomly

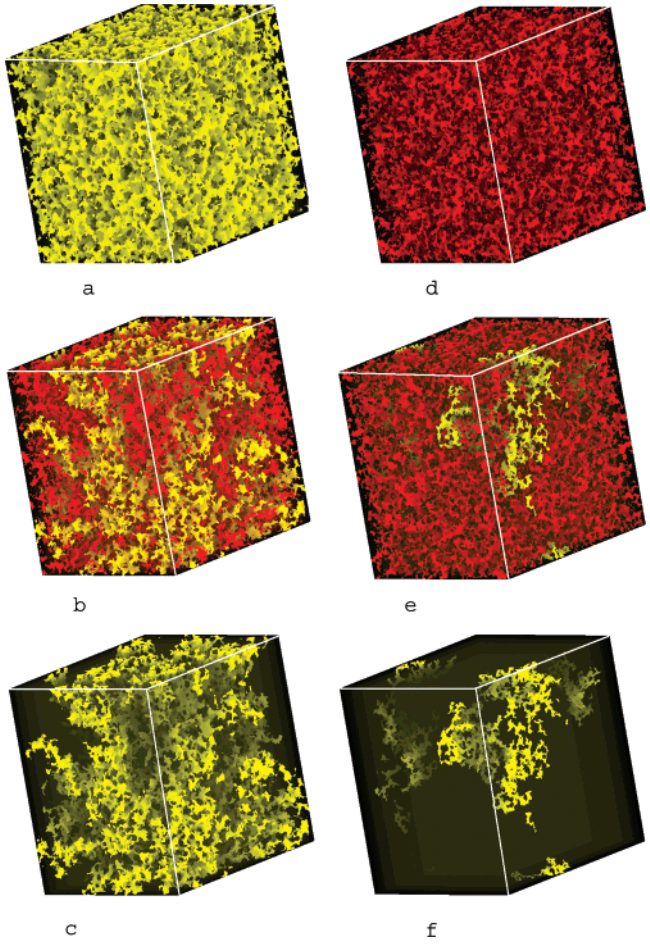

Figure 2. Images of the accessible volume for DLCA gels at different values of ϕ_a. Percolating and isolated pores are indicated in yellow and red, respectively. For clarity, parts c and f show just the percolating pore of systems shown in parts b and e, respectively.

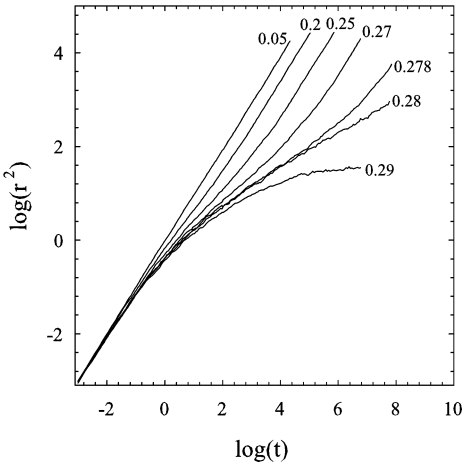

Figure 3. MSD of tracer spheres in DLCA gels of spheres with the same diameter as the tracers at different ϕ, indicated in the figure.

distributed hard spheres and gels formed by DLCA and RLCA. In the latter case, ϕ_a increased with decreasing bond formation probability, but the variation became negligible below 10^{-4}, which we have taken as the RLCA limit. For a given concentration, ϕ_a is larger for RLCA gels than for DLCA gels which in turn is larger than that for the hard sphere system. Gels have a larger ϕ_a value because the particles are connected and therefore have a larger fraction of overlapping excluded volume. ϕ_a is larger for RLCA than DLCA because RLCA clusters are denser.

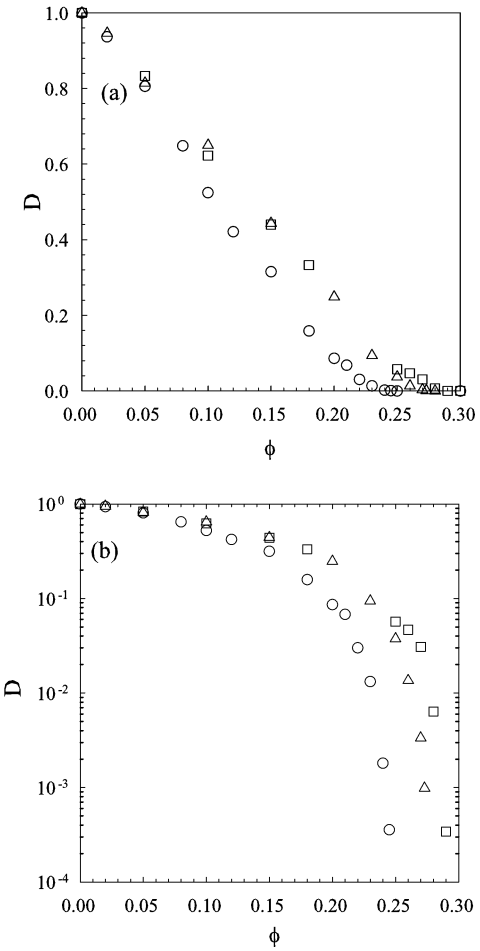

Figure 4. (a) Relative diffusion coefficient of tracer spheres as a function of ϕ in FHS (circles), DLCA (triangles), and RLCA (squares) gels of spheres with the same diameter as the tracers. (b) The same data as part a on a logarithmic scale for D.

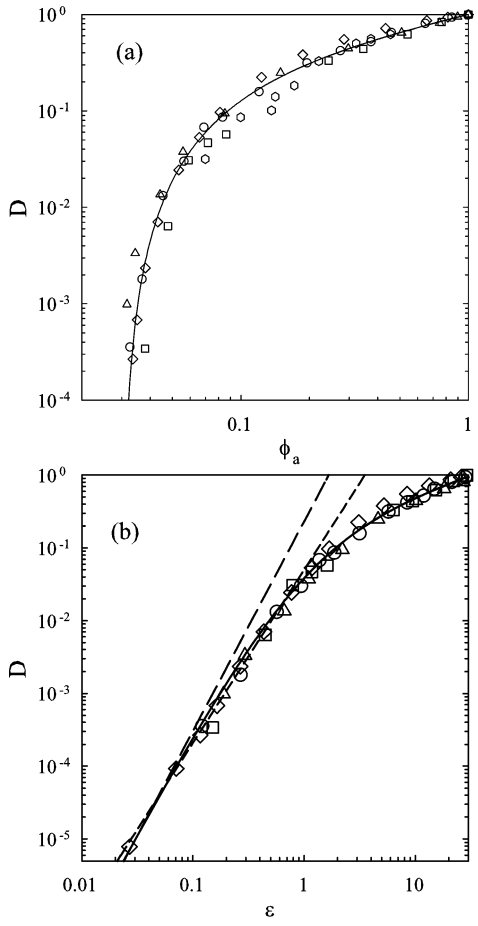

Figure 5. Relative diffusion coefficient of tracer spheres as a function of ϕ_a in FHS (circles), DLCA (triangles), and RLCA (squares) gels of spheres with the same diameter as the tracers. The results for the Lorentz gas[13] (diamonds) and experiments[14] (hexagons) are also shown for comparison. The solid line represents eq 1 where we have used $\phi_a^c = 0.03$ and $\mu = 2.8$. These values were chosen to obtain visually a good description of the data. (b) The same data as part a plotted as a function of $\epsilon = (\phi_a - \phi_a^c)/\phi_a^c$ on a logarithmic scale. The straight lines in part b represent the predicted power law dependences from ref 10 (2.38, short dashed) and ref 11 (2.88, long dashed).

For non-interacting hard spheres, ϕ_a is directly related to the chemical potential (μ_{cs}), $\phi_a = \phi \exp(-\mu_{cs})$,[18] and can be calculated using the so-called Carnahan−Starling equation[19] for μ_{cs}; see the solid line in Figure 1. For randomly distributed hard spheres, the initial dependence of ϕ_a on ϕ is given by $\phi_a = 1 - \phi(1 + b)^3$, where b is the size ratio of the tracers over the obstacles.[8] For gels, the initial dependence can be estimated by assuming that the gels consist of strands of touching spheres: $\phi_a = 1 - \phi(1 + 3b + 1.5b^2)$. The dashed lines in Figure 1 show that these estimates are only valid for small ϕ_a.

Images of the accessible volume in DLCA gels at different ϕ are shown in Figure 2. At low volume fractions (Figure 2a), almost all pores percolate through the system (yellow), but with increasing ϕ (Figure 2b and e) the fraction of finite pores increases until above a critical value (ϕ^c) (Figure 2d) there is no longer a percolating pore. For clarity, we have shown the percolating pore separately in Figure 2c and f.

The MSD averaged over all tracers is shown in Figure 3 for DLCA gels at different ϕ values. The results are similar to those obtained by Höfling et al.[13] for the Lorentz gas. Initially, the tracers diffuse freely until they hit the obstacles. Then, the displacement of tracers is anomalous until $\langle r^2 \rangle$ exceeds a characteristic value (ξ^2) after which it becomes again diffusional with a reduced diffusion coefficient. ξ represents the correlation length of the percolating pores and diverges at the threshold. The correlation length of the pores depends also on the tracer size, see below, and is not related to the correlation length of the gels. The latter decreases with increasing volume fraction and is only a few particle diameters for $\phi > 0.05$.[7] The tracers in finite size pores are trapped and do not contribute to $\langle r^2 \rangle$ at long times. For $\phi > \phi_c$, all of the tracers are trapped and $\langle r^2 \rangle$ stagnates at twice the averaged squared radius of gyration of the pores ($\langle R_g^2 \rangle$). This follows from the fact that the average distance a tracer has moved in a finite size pore at $t \rightarrow \infty$ is the same as the average distance between two randomly placed tracers.

In Figure 4, the dependence on ϕ of the long time diffusion coefficient relative to the free diffusion coefficient (D) is compared for DLCA and RLCA gels and frozen random hard spheres. For a given volume fraction, D is close for the two gels but is smaller for FHS. We note that for systems of freely moving obstacles D decreases much more slowly with increasing ϕ.[20,21] D goes to zero at ϕ_c equal to 0.248 ± 0.003, 0.279 ± 0.001, and 0.295 ± 0.005 for FHS, DLCA, and RLCA, respectively. The error bars indicated the highest fraction where we observed long time diffusion and the lowest fraction where we observed stagnation of MSD.

The same results are plotted as a function of ϕ_a in Figure 5. For comparison, we have included in Figure 5 results obtained for the Lorentz gas.[13] Here, and in ref 11, only the diffusion of tracers in the pores is considered. Other results for the Lorentz

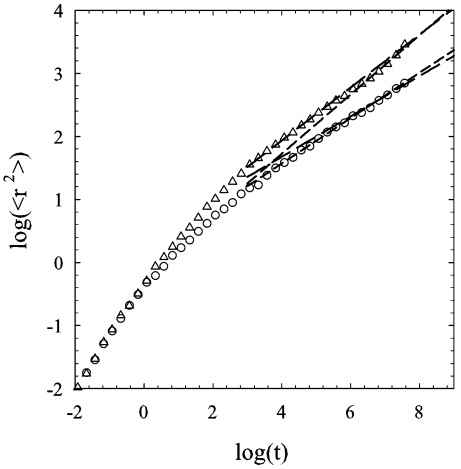

Figure 6. Comparison of the MSD of tracers in a DLCA gel at the percolation threshold of the accessible volume placed anywhere in the accessible volume (circles) or just in the percolating pore (triangles). The straight lines represent the predicted power law dependences in the system and in the percolating pore from ref 10 (short dashed) and ref 11 (long dashed).

gas were obtained in the context of the conductivity that is proportional to point tracer diffusion.[8,22] In these earlier simulations, the average was taken over all tracers including the immobile ones placed in the obstacles so that D was reduced by a factor ϕ_a. After correction, these results are close to the results shown in Figure 5. Experimental results derived from conductivity measurements on fused spherical glass beads in water[14] are close to the simulation results. When ϕ_a approches unity, D should decrease as $\sqrt{\phi_a}$.[23] The full dependence can be described approximately by the following empirical equation which has the predicted limiting behavior for $\phi_a \rightarrow 1$ and $\phi_a \rightarrow \phi_a^c$:

$$D = \sqrt{\phi_a}\left[\frac{\phi_a - \phi_a^c}{\phi_a(1-\phi_a^c)}\right]^{\mu} \qquad (1)$$

with $\phi_a^c = 0.03$ and $\mu = 2.8$; see the solid lines in Figure 5.

It appears that ϕ_a is the parameter that determines the diffusion coefficient for all of these different systems; the variation of ϕ_a for a given D value is less than 20%. In each case, D goes to zero at a critical value (ϕ_a^c) close to 0.03, but the actual value of ϕ_a^c is not universal, as noted earlier by Rintoul.[12] Figure 5b shows the data plotted as a function of the distance to the percolation threshold (ϵ). For the Lorentz gas, we have used the precise value of ϕ_a^c calculated by Rintoul: $\phi_a^c = 0.0301 \pm 0.0003$. For the other systems, we do not have the same precision, but we found that the data superimpose close to ϕ_a^c if we choose $\phi_a^c = 0.029$ for FHS, $\phi_a^c = 0.02655$ for DLCA gels, and $\phi_a^c = 0.033$ for RLCA gels.

The dependence of D close to the percolation threshold is compatible with a power law: $D \propto \epsilon^{\mu}$. However, there is considerable uncertainty in the value of the exponent due to the strong correlation between ϕ_a^c and μ. For instance, Höfling et al.[13] fixed μ at 2.88 predicted by Machta et al.[11] and found in this way $\phi_a^c = 0.0298$. Fixing ϕ_a^c at 0.0301, we find $\mu = 2.5$ using the same data. In fact, the predictions for μ from refs 10 and 11 are both compatible with the data, see Figure 5, and we are not in the position to decide which, if any, is correct. Nevertheless, μ is clearly larger than the value 1.88 obtained from lattice simulations of diffusion in percolating systems.[9]

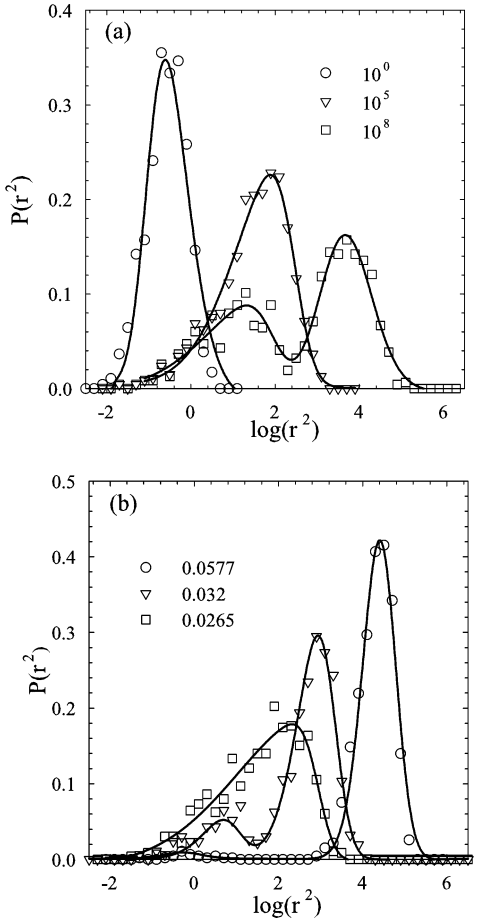

Figure 7. Distribution of the MSD of tracers in a DLCA gel for a fixed value of $\phi_a = 0.0276$ close to the percolation threshold at different times (a) and for a fixed value of $t = 10^6$ at different ϕ_a values (b), as indicated in the figure. The solid lines are guides to the eye.

The power law exponent (k) of the anomalous MSD at the threshold is related to μ as[9] $k = 2(\nu - \beta/2)/(2\nu + \mu - \beta)$, where β characterizes the dependence of the volume fraction of the percolating pores (ϕ_a^p) close to the threshold, $\phi_a^p \propto \epsilon^{\beta}$, and ν characterizes the divergence of the correlation length, $\xi \propto \epsilon^{-\nu}$. If one only considers the displacement of tracers in the percolating pore, the exponent is larger: $k' = 2\nu/(2\nu + \mu - \beta)$. Figure 6 compares the average MSD at the percolation threshold of tracers placed anywhere in the accessible volume with that of tracers placed in the percolating pore. Utilizing the values for $\nu = 0.88$ and $\beta = 0.41$ obtained from lattice simulations[24] gives $k = 0.36$ and $k' = 0.47$ for $\mu = 2.38$ and $k = 0.32$ and $k' = 0.42$ for $\mu = 2.88$. The latter appear to describe the data better, but unfortunately, accurate determination of the limiting power law behavior is largely beyond the current computer capacities, given the fact that the limiting power law behavior of the cluster size distribution is not yet observed even for lattice simulations with a box size of 1023.[25]

The displacement of tracers is highly heterogeneous close to the percolation threshold and can be characterized in terms of the probability distribution that tracers have moved a distance of r^2 at time t ($P(r^2)$). For $\phi_a > \phi_a^c$, we need to distinguish between the fraction (ϕ_a^p) of tracers in the percolating pore and the fraction ($\phi_a - \phi_a^p$) in finite size pores. $P(r^2)$ of tracers in the percolating pores is Gaussian if the MSD is much larger than ξ^2 and $\langle r^2 \rangle$ increases linearly with time. On the other hand, $P(r^2)$ of tracers trapped in a finite size pore becomes independent of t and $\langle r^2 \rangle$ stagnates at $2\langle R_g^2 \rangle$. Therefore, $P(r^2)$ splits up into two

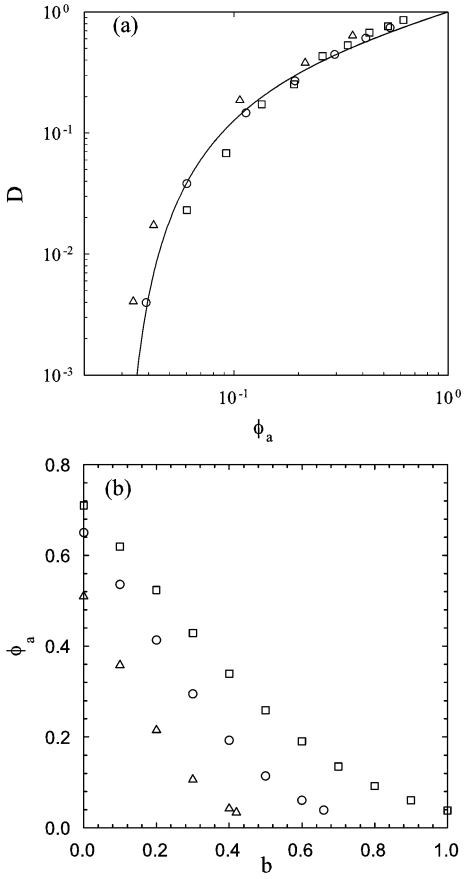

Figure 8. Relative diffusion coefficient of tracer spheres with different diameters between 0.1 and 1 as a function of ϕ_a in FHS at $\phi = 0.35$ (circles), a DLCA gel at $\phi = 0.49$ (triangles), and a RLCA gel at $\phi = 0.29$ (squares) formed by spheres of unit diameter. The solid line is the same as that in Figure 5. (b) The dependence of ϕ_a on the tracer diameter.

peaks: one representing tracers in the percolating pore that displaces linearly with t and another representing tracers in finite size pores that stagnates, with relative amplitudes ϕ_a^p and $(\phi_a - \phi_a^p)$, respectively. The split-up is illustrated in Figure 7a where $P(r^2)$ is shown at three times for a DLCA gel just above the percolation threshold ($\phi_a = 0.0276$). At the shortest time, the MSD is still much smaller than ξ^2, and one observes a single distribution. The split-up starts when $\langle r^2 \rangle \approx \xi^2$ and is clearly visible at the longest time when $\langle r^2 \rangle$ is much larger than ξ^2. Figure 7b shows the distributions at $t = 10^6$ for three values of ϕ_a. At $\phi_a = 0.0265$, that is, smaller than ϕ_a^c, only one peak is observed representing the pore size distribution, which is broad close to the threshold. At $\phi_a = 0.056$, almost all accessible volume percolates and a narrow peak is seen that shifts to larger r^2 with time. For $\phi_a = 0.032$, that is, just above ϕ_a^c, both peaks representing freely diffusing and trapped tracers are observed.

The same features were found when ϕ_a was varied by varying the tracer size at constant obstacle volume fraction. As mentioned above, ϕ_a decreases with increasing tracer size starting from $\phi_a = 1 - \phi$ for point tracers; see Figure 8b. Examples of the dependence of D on ϕ_a are given in Figure 8a for different tracer diameters between 0.1 and 1 for gels and FHS at fixed volume fractions. Diffusion coefficients obtained at other volume fractions showed the same universal behavior. For the Lorentz gas, there is a strict equivalence between the diffusion of point tracers and finite size tracers at the same ϕ_a.[8] Similar equivalence exists between finite size tracers in FHS and point tracers in randomly distributed semipenetrable spheres. It was found, for a limited range of ϕ_a, that D was the same for a given ϕ_a value for tracers with different sizes in FHS.[8] Figure 8 shows that the effect of tracer size on D is essentially determined by ϕ_a also for gels, but the relationship is not exact.

IV. Conclusion

The most important result of the simulations presented here is that the diffusion coefficient in a system of immobile noninteracting obstacles is determined by the volume that is accessible to the tracers independent of the tracer size. We have found this to be true for two different gel structures but also for frozen hard spheres and for the Lorentz gas. This point has so far not been considered in existing theories on tracer diffusion in gels.

The tracer diffusion becomes zero at a critical value of accessible volume, $\phi_a^c \approx 0.03$, that is almost the same for gels and frozen hard spheres. The dependence of D on ϕ_a close to ϕ_a^c can be described in terms of a power law dependence on the distance to ϕ_a^c. The MSD at ϕ_a^c is anomalous and increases as a power law with time with an exponent less than unity. The exponents of the two power law relationships are related and are consistent with the percolation model.

In principle, the diffusion coefficient can be predicted with reasonable accuracy if the gel structure is known and ϕ_a can be calculated. Unfortunately, the reverse case, that is, deducing the gel structure from a measurement of the diffusion coefficient, is not as straightforward because the relation between ϕ_a and the structure is not direct. Nevertheless, the validity of postulated gel structures may be tested by measuring diffusion coefficients of tracers with different size.

A different relation between D and ϕ_a is expected when the bonds between the obstacle particles are flexible or when they interact with the tracers. These effects can be tested with the same simulation method and will be reported in the future.

Acknowledgment. This work has been supported in part by a grant from the Marie Curie Program of the European Union numbered MRTN-CT-2003-504712.

References and Notes

(1) Nicolai, T. In *Food Colloids Self-Assembly and Material Sciences*; Dickinson, E., Leser, M. E., Eds.; The Royal Society of Chemistry: Cambridge, 2007; pp 35−56.
(2) Nicolai, T.; Cocard, S. *Eur. Phys. J. E* **2001**, *5*, 221−227.
(3) Chen, S. H.; Rouch, J.; Sciortino, F.; Tartaglia, P. *J. Phys.: Condens. Matter* **1994**, *6*, 10855−10883.
(4) Poon, W. C. K.; Haw, M. D. *Adv. Colloid Interface Sci.* **1997**, *73*, 71−126.
(5) Trappe, V.; Sandkuhler, P. *Curr. Opin. Colloid Interface Sci.* **2004**, *8*, 494−500.
(6) Rottereau, M.; Gimel, J. C.; Nicolai, T.; Durand, D. *Eur. Phys. J. E* **2004**, *15*, 133−140.
(7) Rottereau, M.; Gimel, J. C.; Nicolai, T.; Durand, D. *Eur. Phys. J. E* **2004**, *15*, 141−148.
(8) Kim, C. I.; Torquato, S. *J. Chem. Phys.* **1992**, *96*, 1498−1503.
(9) Havlin, S.; Ben-Avraham, D. *Adv. Phys.* **1987**, *36*, 695−798.
(10) Halperin, B. I.; Feng, S.; Sen, P. N. *Phys. Rev. Lett.* **1985**, *54*, 2391−2394.
(11) Machta, J.; Moore, S. M. *Phys. Rev. A* **1985**, *32*, 3164−3167.
(12) Rintoul, M. D. *Phys. Rev. E* **2000**, *62*, 68−72.
(13) Höfling, F.; Franosch, T.; Frey, E. *Phys. Rev. Lett.* **2006**, *96*, 165901−165904. Here, the results are given in terms of the obstacle number density (n) which is related to ϕ_a as $\exp(-(4/3)\pi n)$.
(14) Roberts, J. N.; Schwartz, M. L. *Phys. Rev. B* **1985**, *31*, 5990−5997.
(15) Weitz, D. A.; Huang, J. S. *Phys. Rev. Lett.* **1985**, *54*, 1416−1419.
(16) Prasad, V.; Semwogerere, D.; Weeks, E. R. *J. Phys.: Condens. Matter* **2007**, *19*, 113102−113125.

(17) Price, W. S. *Cur. Opin. Colloid Interface Sci.* **2006**, *11*, 19−23.
(18) Frenkel, D.; Smit, B. *Understanding Molecular Simulation: From Algorithms to Applications*; Academic: San Diego, CA, 2002.
(19) Carnahan, F. N.; Starling, E. K. *J. Chem. Phys.* **1969**, *51*, 635−636.
(20) Moriguchi, I. *J. Chem. Phys.* **1997**, *106*, 8624−8625.
(21) Babu, S.; Gimel, J. C.; Nicolai, T. *J. Chem. Phys.* **2007**, *127*, 054503.
(22) Tobochink, J.; Laing, D.; Wilson, G. *Phys. Rev. A* **1990**, *41*, 3052−3058.
(23) Torquato, S. *Random Hetergeneous Materials: Microstructure and Macroscopic Properties*; Springer: New York, 2001.
(24) Stauffer, D.; Aharony, A. *Introduction to Percolation Theory*, 2nd ed.; Taylor and Francis: London, 1992.
(25) Gimel, J. C.; Nicolai, T.; Durand, D. *J. Phys. A: Math. Gen.* **2000**, *33*, 7687−7697.